We are IntechOpen, the world's leading publisher of Open Access books Built by scientists, for scientists

4,800
Open access books available

122,000
International authors and editors

135M
Downloads

Our authors are among the

154
Countries delivered to

TOP 1%
most cited scientists

12.2%
Contributors from top 500 universities

CLARIVATE ANALYTICS BOOK CITATION INDEX INDEXED

WEB OF SCIENCE™

Selection of our books indexed in the Book Citation Index in Web of Science™ Core Collection (BKCI)

Interested in publishing with us?
Contact book.department@intechopen.com

Numbers displayed above are based on latest data collected.
For more information visit www.intechopen.com

Chapter 8

A Process for Preparing High Graphene Sheet Content Carbon Materials from Biochar Materials

Yan-Jia Liou and Wu-Jang Huang

Additional information is available at the end of the chapter

http://dx.doi.org/10.5772/61200

Abstract

Graphene is monolayer graphite and has higher electron mobility than silicon, high heat conduction, and special optical properties. In this study, we have attempted to use a two-step process (an acid pretreatment followed by a heat treatment) for producing high graphene sheet content (>80%) carbon materials (GSCCMs) from monocotyledonous and dicotyledonous biochar materials prepared at 350°C. The highest graphene sheet content of 83.86% is found with the CH_3COOH pretreatment followed by a 1500°C heat treatment of monocotyledonous biochar materials, and its conductivity was measured at 84.69 S/cm. Therefore, preparing GSCCMs from biochar materials could highly reduce the cost.

Keywords: Fullerenes, oxides, biomaterials, IR

1. Introduction

Graphene is monolayer graphite and has higher electron mobility than silicon, high heat conduction, and special optical properties. Graphene is composed of two-dimensional and hexagonal rings of sp^2 carbon atoms. The potential graphene application includes photoelectric elements, various medical applications, adsorbents for environmental pollutants, and use as a semiconductor material. The researchers used graphene as a transparent conductive oxide thin film. The results show that the electron and hole mobilities of the device are 1100 ± 70 cm^2/Vs and 550 ± 50 cm^2/Vs at the drain bias of –0.75 V, respectively [1]. In 2008, Hong et al. [2] mixed graphene and polyethylene dioxythiophene doped with polystyrene sulfonic acid

(PEDOT-PSS) to make dye-sensitized solar cells (DSSC). The results show that the optimal efficiency of photoelectric conversion is 4.5%. Hollanda et al. [3] mixed graphene and CNTs to make a nanocomposite as a gene transfection. The results show that the graphene/CNT nanocomposite has moderate to low cytotoxicity, high-transfection efficiency, and great potential as a gene carrier agent in nonviral-based therapy. In 2014, Sheshmani et al. [4] used magnetic graphene/chitosan for the removal of acid orange 7. From the results, it was found that the magnetic graphene/chitosan can effectively remove the anionic azo dyes from wastewater. Researchers' evaluations of graphene as an adsorbent for solid phase extraction with chlorophenols when applied to the analysis of river water samples had recoveries above 77.2% [5].

Many manufacturing methods of graphene have been proposed, such as chemical vapor deposition [6], chemical reduction of graphene oxide [7, 8], and exfoliation method [9]. In several studies, researchers have used a combined ozone–oxidation with annealing at 530 K to produce graphene powders from highly oriented pyrolytic graphite [10]. In 2010, Akhavan [11] used graphene oxide prepared graphene thin film through heat treatment. The results show that it can form a thickness of graphene thin film of 0.37 nm at 1000°C.

However, these processes are complicated by a high cost and the difficulty of removing by-products. Therefore, the market mechanisms of graphene have not yet been established at present. The authors have always used a low temperature and two-step pyrolized process in the production of graphene content carbon material from woody wastes. The first step is the charring process of biomass into biochar; the secondary step is to form graphene microcrystals by heating up to 1400°C. The results have shown that the most used secondary pyrolysis temperature at 1400°C has made graphene content carbon materials; the content of the graphene sheet was measured at 62.47%. In another work, we have found that the production of graphene content carbon from woody materials created a surface Raman quenching phenomenon [12, 13] (see Figures S2 and S3). In this study, we would like to report a modified process for directly preparing high graphene sheet content carbon materials (GSCCMs) from biochar materials.

2. Experimental

2.1. Preparation of biochar materials

In this study, biomass materials were sampled from the monocotyledonous materials (such as *Cocos nucifera*, *Elaeis guineensis Jacq*, and *Kingia australis*) and dicotyledonous materials (such as *Cinnamomum camphora*, *Cryptomeria japonica*, and *Aextoxicon punctatum*). The dicotyledonous biomass (*C. japonica*) was dried and cut into smaller pieces with dimensions of 5 × 2 × 4 mm^3 in length, width, and height, respectively. The monocotyledonous biomass (*E. guineensis Jacq.*) was cut into smaller pieces with dimensions of 2 × 0.05–0.2 × 0.05–0.2 mm^3 in length, width, and height, respectively. The biomass materials were heated at 350°C for 1 h to convert them into biochar materials. *E. guineensis Jacq.* and *C. japonica* were selected due to there are common woody materials in Taiwan.

2.2. Preparation of Graphene Sheet Content Carbon Materials (GSCCMs)

A two-step process with an acid pretreatment followed by a heat treatment produced high graphene sheet content carbon materials (GSCCMs) from monocotyledonous and dicotyledonous biochar materials. In the first acid pretreatment step, the above-mentioned biochar materials were immersed in 5 M of sulfuric acid (H_2SO_4) solution and 5 M of acetic acid (CH_3COOH) solution at room temperature for 14 days, respectively. After acid pretreatment, biochars were dried at 105 ± 5°C before they were heated at 500°C, 800°C, 1200°C, and 1500°C under a vacuum.

The IDs of dicotyledonous samples are denoted as SC500, SC800, SC1200, and SC1500 (H_2SO_4 pretreatment), as well as AC500, AC800, AC1200, and AC1500 (CH_3COOH pretreatment), respectively. The IDs of monocotyledonous samples are denoted as SE500, SE800, SE1200, and SE1500 (H_2SO_4 pretreatment), as well as AE500, AE800, AE1200, and AE1500 (CH_3COOH pretreatment), respectively.

2.3. Property analysis of samples

An S-3000N (HITACHI, Japan) scanning electron microscope meter equipped with an energy dispersive spectrometer (SEM/EDX) was applied to analyze the structural exterior of the prepared GSCCM products. A Vector22 (Bruker, Germany) Fourier transform infrared spectrometer (FT-IR) was used to analyze their functional groups. A D8 Advance (Bruker, Germany) X-ray diffractometer (XRD) was used to analyze the lattice structures, and an FPSR-100 (Solar Energy Tech, Taiwan) four-point sheet resistance meter was used to analyze the samples' resistivity and conductivity.

3. Results and discussion

Figures 1 to 3 show the SEM image of GSCCM samples; surface erosion and the formation of graphite spherical grains are observed for biochar materials after acid pretreatment and heat treatment, respectively. The temperature necessary to generate a large number of graphite spherical grains was found to begin at 800°C. When the heating temperature was raised to 1500°C, the size of graphite spherical grains is increased. The authors' other publication had found that sodium ions have more contribution on the formation of those graphite spherical grains [14] (see Figure S4).

The FT-IR spectra of acid-pretreated dicotyledonous biochar materials are shown in Figure 4a, and those of monocotyledonous biochar materials are shown in Figure 4b. Both have amide groups (~3850 and 3745 cm^{-1}), aromatic groups (~ 878, 650 and 590 cm^{-1}), –OH (~3500 cm^{-1}), –CH_2- (~2950 cm^{-1}), C=O (~1630 cm^{-1}), –CH_3 (~1397 cm^{-1}), and C-O (~1100 cm^{-1}) stretching vibration motion. The peaks are from the cellulose and lignin structure of plants and corresponded to the peak of absorbed CO_2 molecules at 2250 cm^{-1}. After H_2SO_4 and CH_3COOH pretreatment, the peak at 1600 cm^{-1} split into outside-C=O and inside-C=O stretching vibration motion in the carbon layers, the peak of –CH_3 disappeared, and the peak at 1700 cm^{-1}

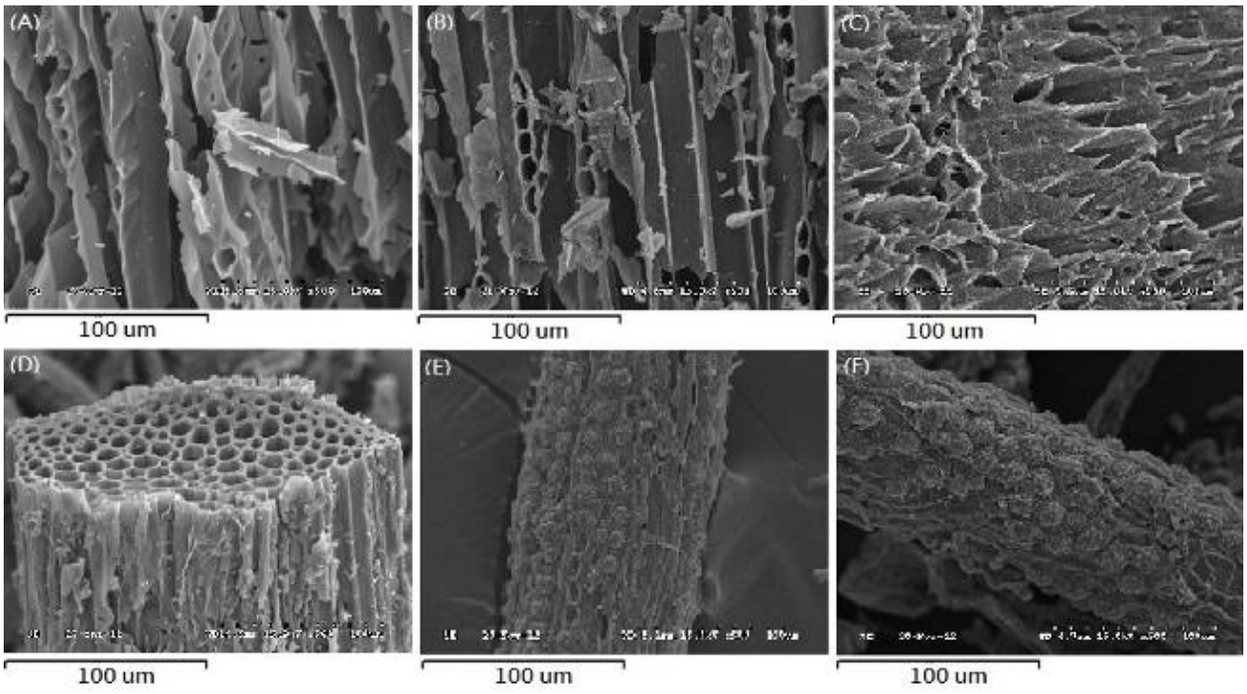

Figure 1. SEM image of (A) dicotyledonous biochar and after acid pretreatment for (B) H_2SO_4 and (C) CH_3COOH and (D) monocotyledonous biochar and after (E) H_2SO_4 and (F) CH_3COOH pretreatment.

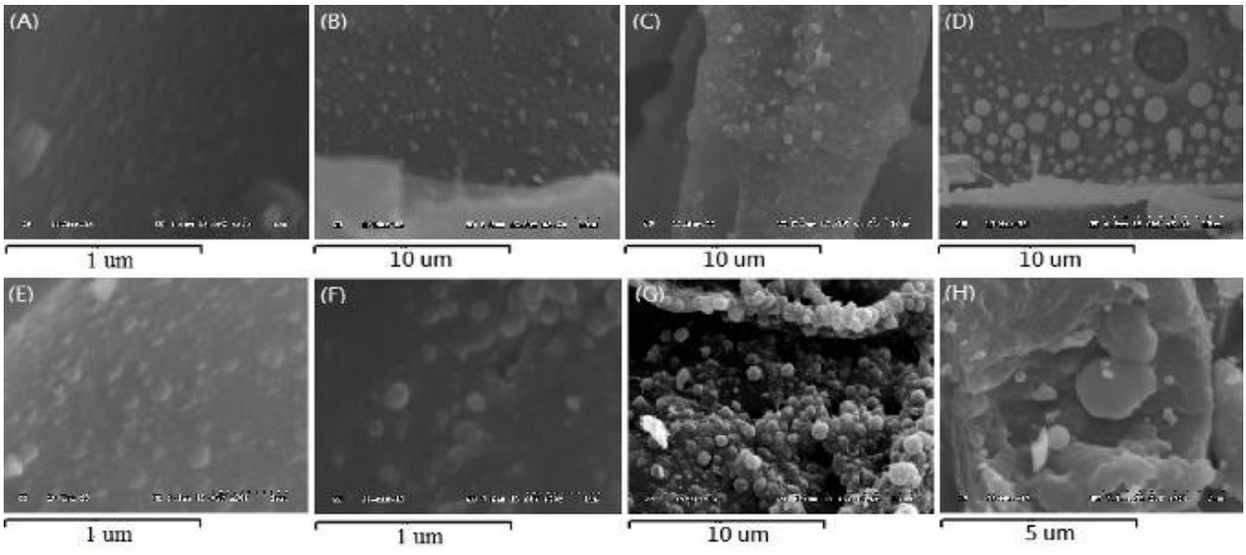

Figure 2. SEM image of GSCCMs of (A) SC500, (B) SC800, (C) SC1200, (D) SC500, (E) SE500, (F) SE800, (G) SE1200, and (H) SE1500.

corresponding to oxide layers was formed. The phenomenon can be attributed to oxidation in part of the carbon structure that converts to epoxy groups. The FT-IR spectra of our produced GSCCMs are shown in Figures 5 and 6. Compared with Figure 4, only peaks at 1700 to 1550 cm^{-1} and 878 to 590 cm^{-1} have been changed significantly with the changing of the heat-treatment temperatures.

http://dx.doi.org/10.5772/61200

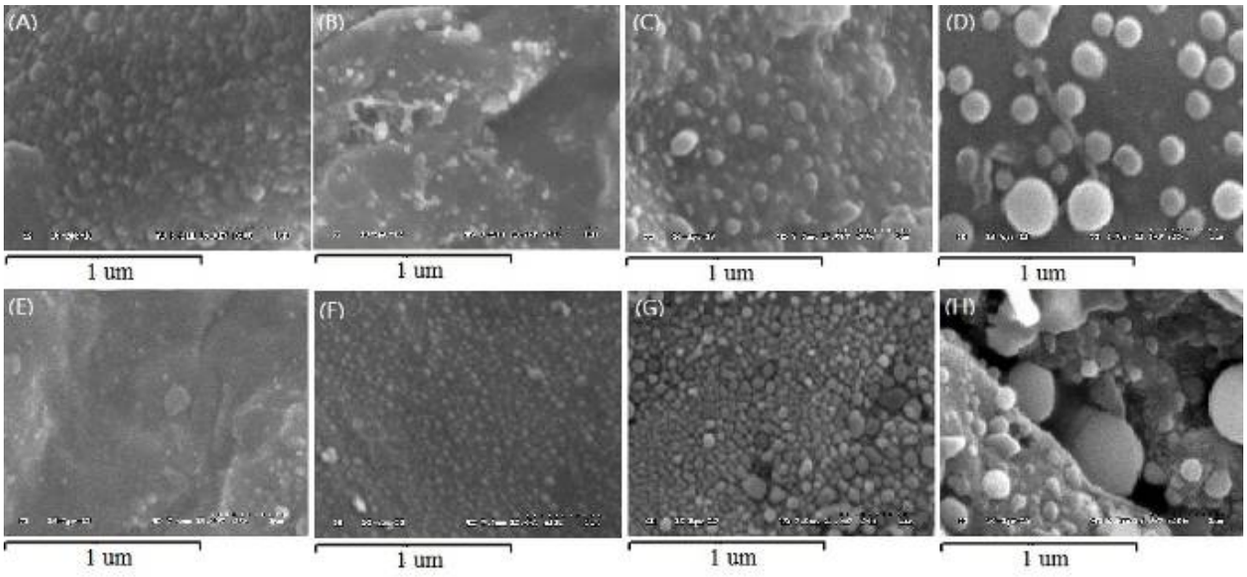

Figure 3. SEM image of GSCCMs of (A) AC500, (B) AC800, (C) AC1200, (D) AC500, (E) AE500, (F) AE800, (G) AE1200, and (H) AE1500.

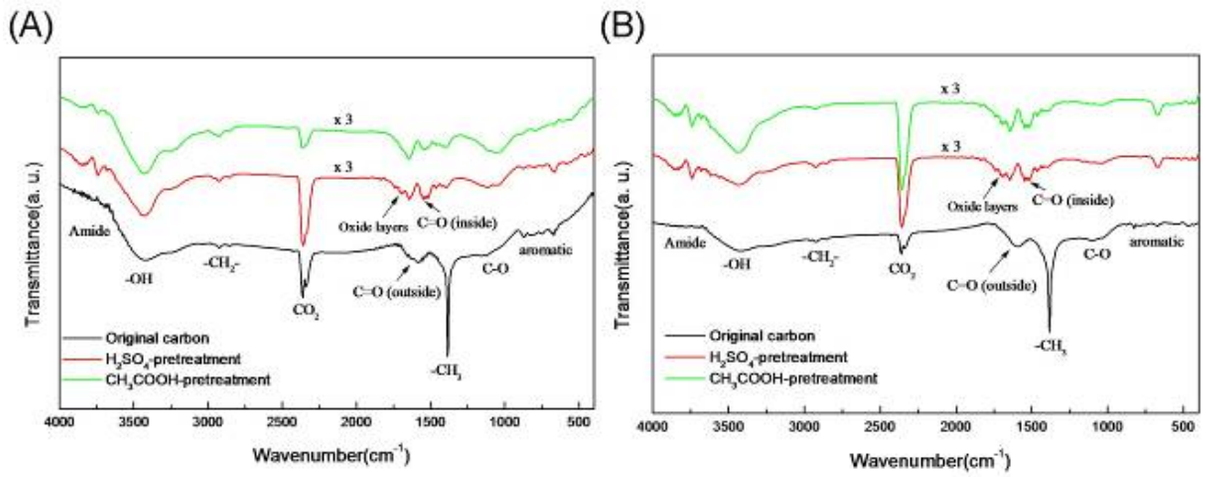

Figure 4. FT-IR spectrums of (A) dicotyledonous and (B) monocotyledonous biochars after acid pretreatment before heat treatment.

Figures 7–9 show the XRD spectrometry analysis results. The biochar and GSCCM samples have a peak of cellulose at around 2θ degree = 22°, at around 2θ degree = 26° (d_{002}), 41° (d_{100}), and 44° (d_{101}) corresponding with crystals of graphite, and a peak at around 2θ degree = 31° corresponding with crystals of C_{60}. The peak (2θ degree = 22°) has an obvious decrease in the intensity. This phenomenon is attribute to the disintegration of cellulose during the acid pretreatment process and the formation of graphitic crystals and oxide layers (2θ degree = 29°) in the GSCCM samples.

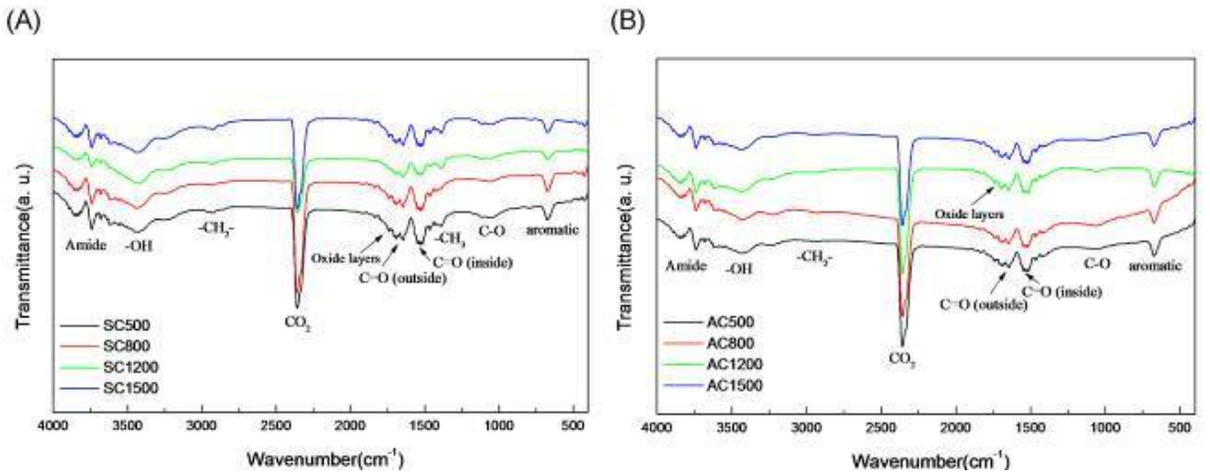

Figure 5. FT-IR spectrums of GSCCMs of the H_2SO_4 pretreated (A) dicotyledonous and (B) monocotyledonous biochars and heat-treated at various temperatures.

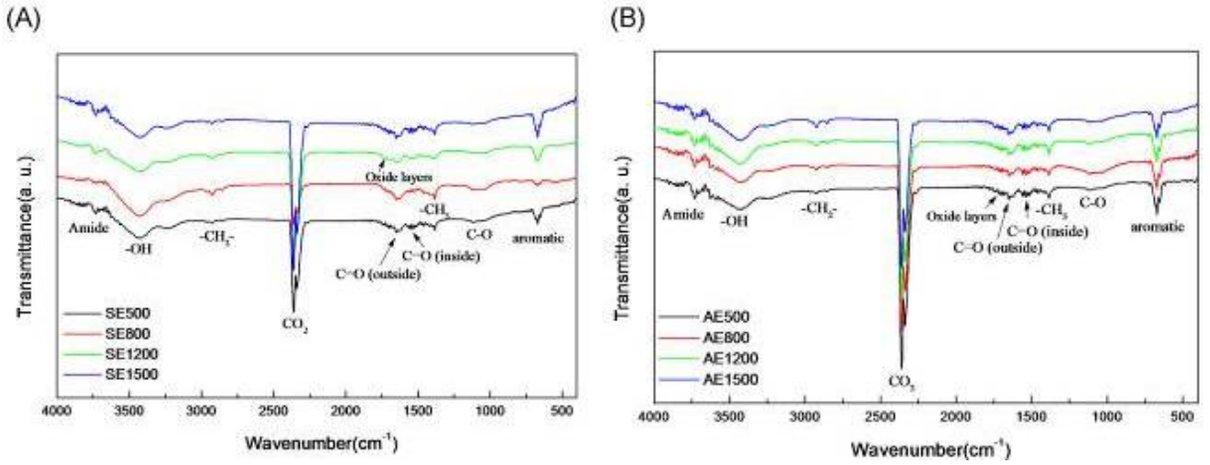

Figure 6. FT-IR spectrums of GSCCMs of the CH_3COOH pretreated (A) dicotyledonous and (B) monocotyledonous biochars after heat-treated at various temperatures.

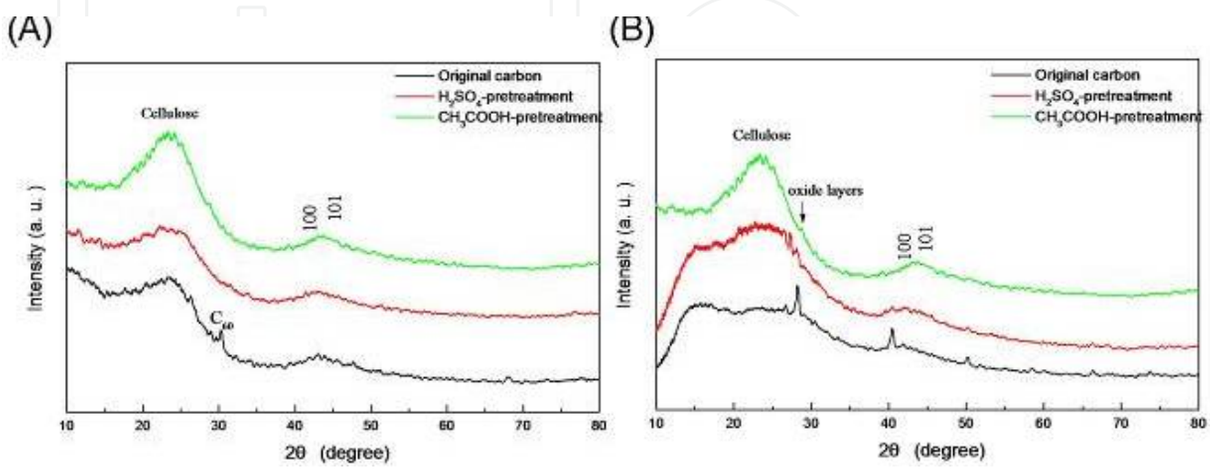

Figure 7. XRD spectrums of (A) dicotyledonous and (B) monocotyledonous biochars after acid pretreatment before heat treatment.

http://dx.doi.org/10.5772/61200

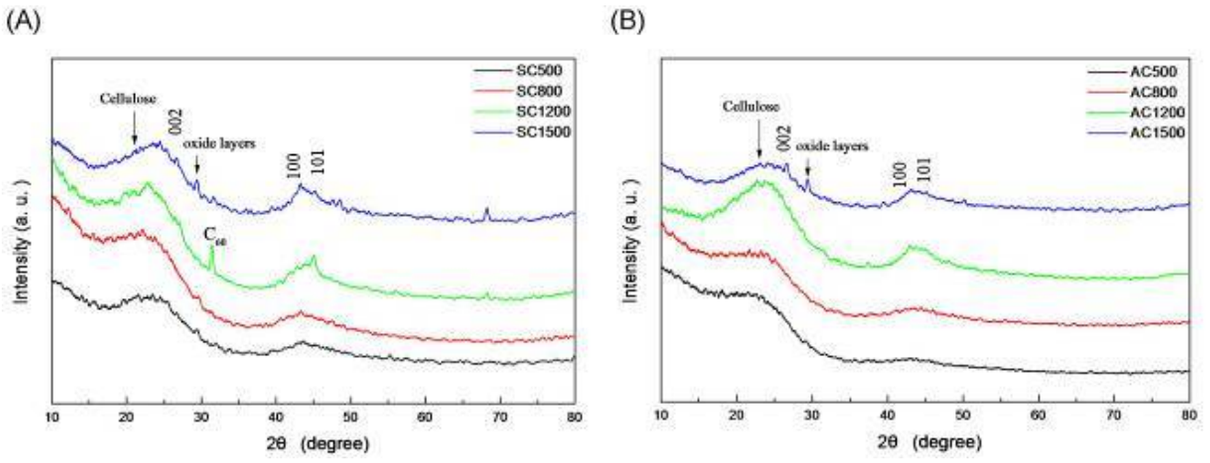

Figure 8. XRD spectrums of GSCCMs of the H_2SO_4 pretreated (A) dicotyledonous and (B) monocotyledonous biochars and heat-treated at various temperatures.

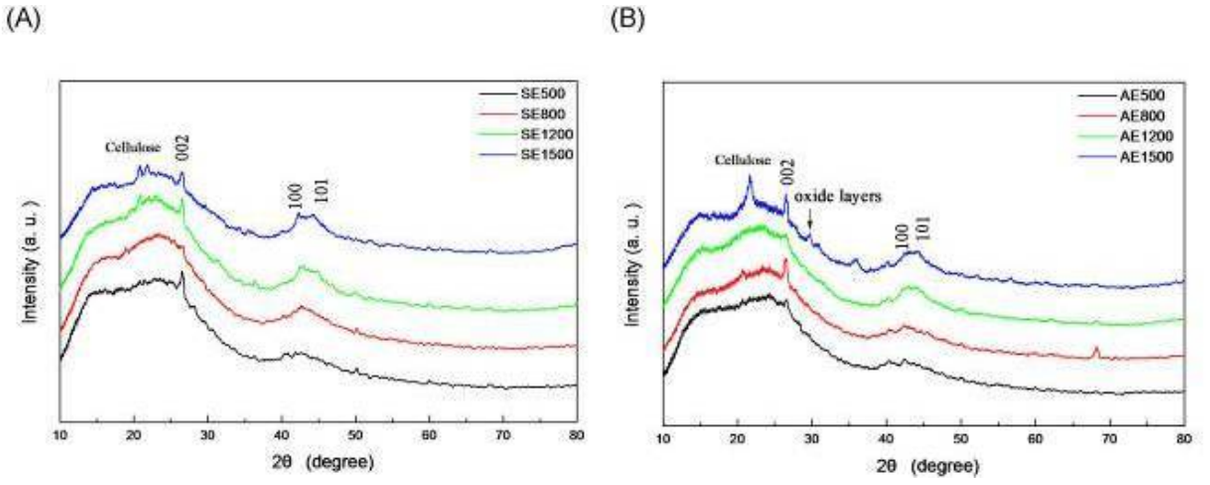

Figure 9. XRD GSCCMs of the CH_3COOH pretreated (A) dicotyledonous and (B) monocotyledonous biochars and heat-treated at various temperatures.

The graphene sheet content of produced GSCCM samples can be characterized quantitatively, according to the author's previous report [12]. Results are shown in Table 1, the GSCCMs, through the two-step processes from biochars, have an increment on the graphene sheet content of 16% to 28% more than that of the two-step heat-treatment-only process from woody biomass [15]. The highest graphene sheet content was found with CH_3COOH and H_2SO_4 pretreatment followed by 1500°C heat-treated monocotyledonous biochar materials; and its average conductivity was measured as 84.69 and 75.55 S/cm, respectively. The total metal content in our synthesized GSCCMs was almost less than 1 wt%, and its contribution to conductivity could be ignored (data not shown here).

According to the industry reports [16], the cost of artificial graphite and graphene for the CVD process is 1450 USD/ton and 28.57 USD/g, respectively. The production cost of GSCCMs was

Biomass	Dicotyledonous				Monocotyledonous			
Preparation method	A) Two stepwise heat treatment processes (without catalytic) [14] from woody biomass B) Two stepwise heat treatment processes (with catalytic) [14] from woody biomass C) Two-step process (H_2SO_4 pretreatment followed heat treatment) from biochar D) Two-step process (CH_3COOH pretreatment followed heat treatment) from biochar							
Method type	A	B	C	D	A	B	C	D
Graphene sheet content (%)								
500°C	18.65	24.66	22.29	25.14	10.08	28.80	22.34	22.56
800°C	23.62	26.08	25.69	25.09	25.00	32.00	36.87	30.61
1200°C	32.96	43.04	43.17	48.61	44.60	50.20	42.13	67.54
1500°C	56.06	62.08	63.12	72.18	80.60	81.20	79.71	83.86
Average conductivity (S/cm)								
500°C	0.01	0.17	0.12	0.14	0.03	0.27	0.28	0.01
800°C	1.24	0.98	0.19	0.13	0.06	0.81	0.93	0.52
1200°C	23.67	24.16	23.01	31.58	30.15	39.54	29.95	61.29
1500°C	50.01	53.31	59.02	66.45	79.08	82.40	75.55	84.69

Table 1. Electrical and graphene sheet content analysis of GSCCMs samples

about 13.33 TND/batch. Therefore, preparing GSCCMs from biochar materials could highly reduce the cost and could be applied in transparent conductive thin film, dry-sensitized solar cells, super capacitors, and composites.

4. Conclusions

According to our results, the highest graphene sheet content of 83.86% is found with the CH3COOH pretreatment followed by a 1500°C heat treatment of monocotyledonous biochar materials, and its conductivity was measured at 84.69 S/cm. Therefore, preparing GSCCMs from biochar materials could highly reduce the cost and could be applied in transparent conductive thin film, dry-sensitized solar cells, super capacitors, and composites.

http://dx.doi.org/10.5772/61200

Supplementary materials

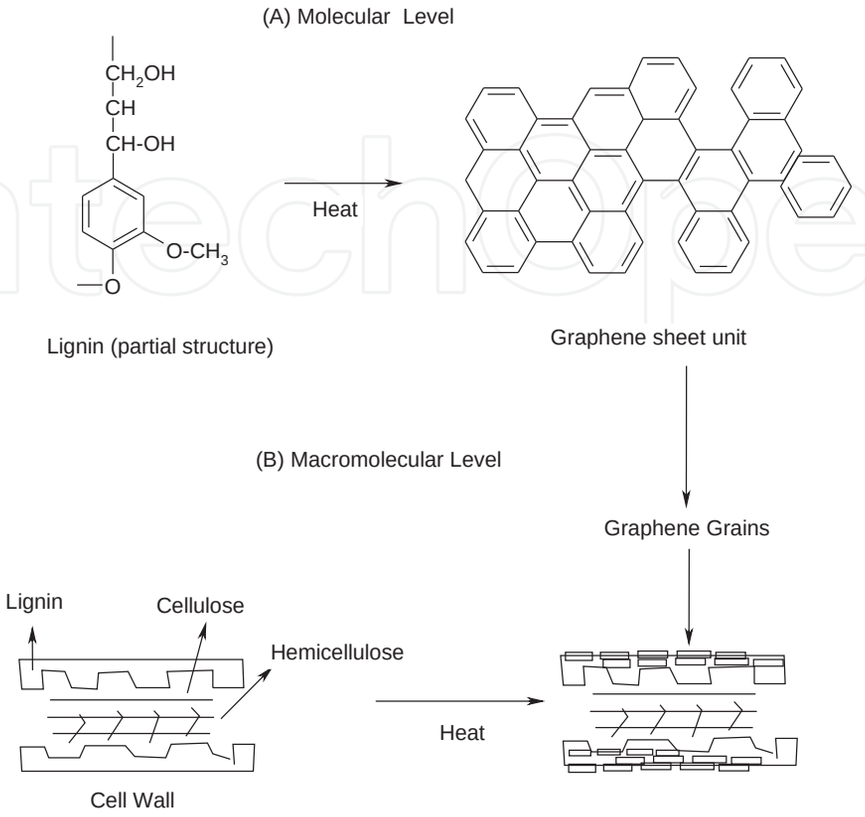

Figure S1. Proposed formation mechanism of graphene grains on cytoskeleton surface of wood cells. (Y. J. Liou, W. J. Huang. Relationship between the formation of graphene fraction and the development of surface electro-conductivity of pyrolized monocotyledonous and dicotyledonous plants. *J. Cryst. Growth,* Under review.)

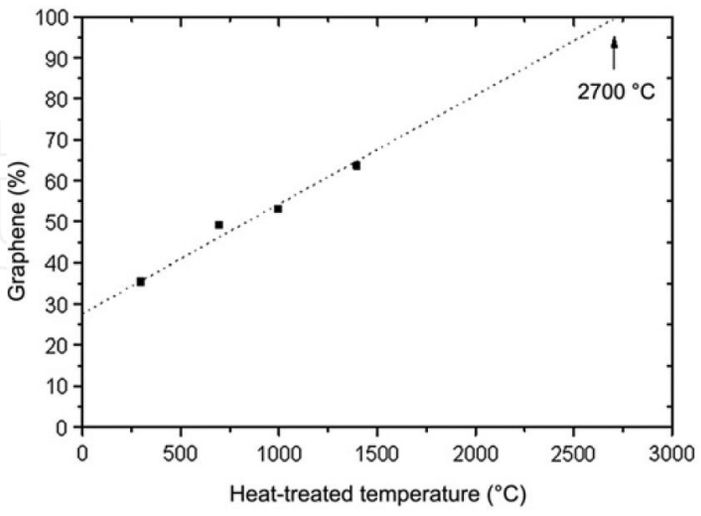

Figure S2. Plot of graphene content and heat-treated temperature of pyrolized wood char powders. (Y. J. Liou, W. J. Huang. Quantitative analysis of graphene sheet content in wood char powders during secondary graphitization. *J. Mater. Sci. Technol.*, 2013, 29: 406.)

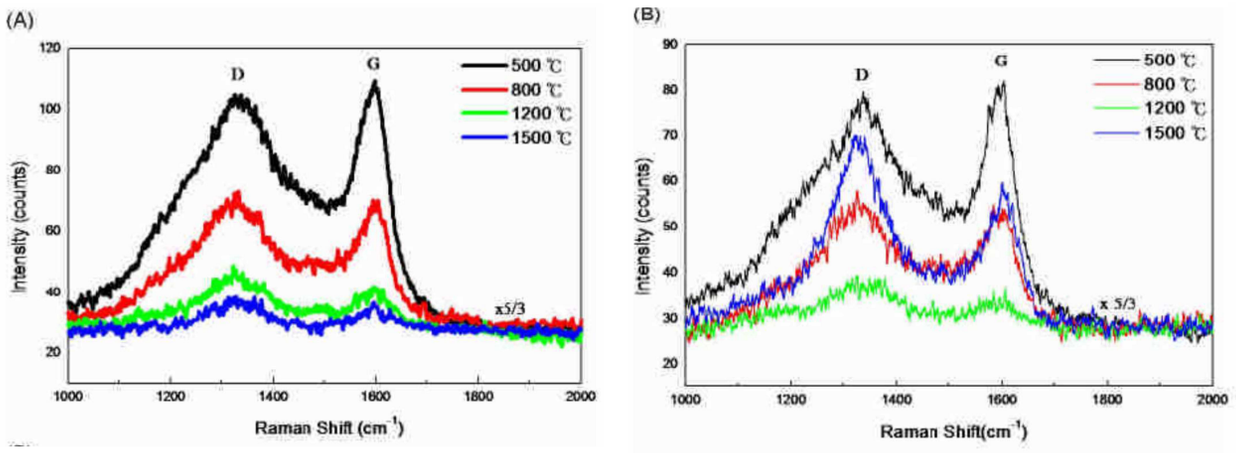

Figure S3. Raman spectrums of graphene sheet content carbon materials by (A) noncatalytic and (B) catalytic pyrolized processes. (Y. J. Liou, W. J. Huang. Determination of graphene sheets content in carbon materials by Raman spectroscopy. *J. Chin. Chem. Soc.* 2014, 61: 1045.)

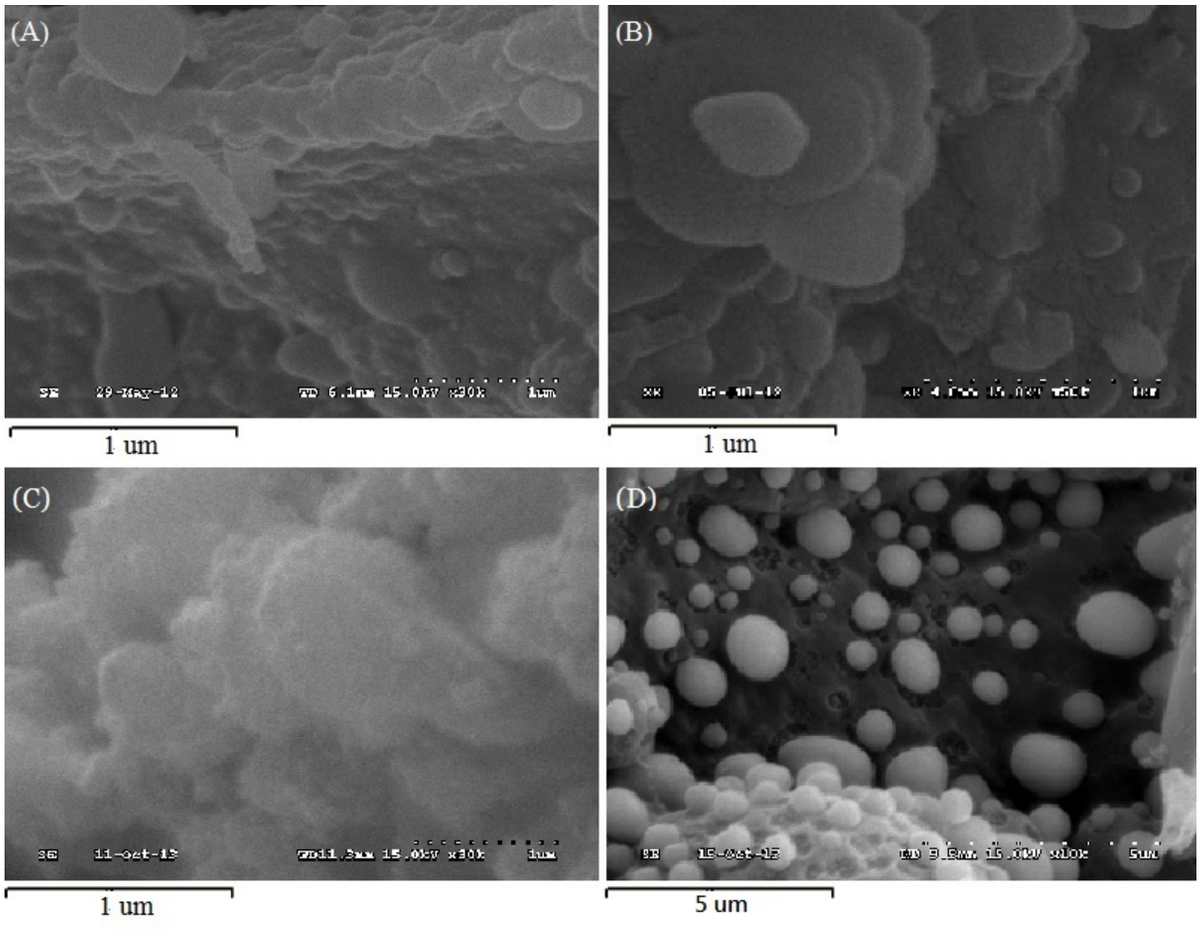

Figure S4. SEM image of GSCCMs by (A) noncatalytic, (B) MnO_2, (C) Li_2O, and (D) Na_2O catalytic pyrolized processes at 1500°C. (Yan-Jia Liou, Wu-Jang Huang. The role of sodium ions on the development of micro-sized pores in a high alpha-cellulose content woody biomass under ambient temperature. J. Cleaner Product. 2014, 47: 199.)

Author details

Yan-Jia Liou and Wu-Jang Huang*

*Address all correspondence to: wjhuang@mail.npust.edu.tw

Department of Environmental Engineering and Science, National Ping-Tung University of Science and Technology, Ping-Tung County, Taiwan

References

[1] Y. Lee, S. Ba, H. Jang, S. Jang, et al. Wafer-scale synthesis and transfer of graphene films. *Nano Lett.*, 2010, 10: 490.

[2] W. Hong, Y. Xu, G. Lu, G. Shi, et al. Transparent graphene/PEDOT-PSS composite films as counter electrodes of dye-sensitized solar cells. *Electrochem. Commun.*, 2008, 10: 1555.

[3] L. M. Hollanda, A. O. Lobo, M. Lancellotti, E. Berni, et al. Graphene and carbon nanotube nanocomposite for gene transfection. *Mater. Sci. Eng. C*, 2014, 39: 288.

[4] S. Sheshmani, A. Ashori, S. Hasanzadeh. Removal of acid orange 7 from aqueous solution using magnetic graphene/chitosan: a promising nano-adsorbent. *Int. J. Biol. Macromol.*, 2014, 68: 218.

[5] Q. Liu, L. Shi, L. Zeng, T. Wang, et al. Evaluation of graphene as an advantageous adsorbent for solid-phase extraction with chlorophenols as model analytes. *J. Chromatogr. A*, 2011, 1218: 197.

[6] J. J. Lu, B. W. Qiu, K. P. Huang, Z. Z. Chang. Large-area synthesis of grapheme monolayer by chemical vapor deposition. *J. Mac. Ind.*, 2010, 326: 103.

[7] X. Shen, L. Jiang, Z. Ji, J. Wu, et al. Stable aqueous dispersions of graphene prepared with hexamethylenetetramine as a reductant. *J. Coll. and Int. Sci.* 2011, 354: 493.

[8] K. S. Novoselov, A. K. Geim, S. V. Morozov, D. Jiang, et al. Electric field effect in atomically thin carbon films. *Science*. 2004, 306(5695): 666.

[9] A. K. Geim. Graphene: status and prospects. *Science.* 2009, 324: 1530.

[10] M. J. Webb, P. Palmgren, P. Pal, O. Karis, et al. A simple method to produce almost perfect graphene on highly oriented pyrolytic graphite. *Carbon,* 2011, 49: 3242.

[11] O. Akhavan. The effect of heat treatment on formation of graphene thin films from graphene oxide nanosheets. *Carbon,* 2010, 48: 509.

[12] Y. J. Liou, W. J. Huang. Quantitative analysis of graphene sheet content in wood char powders during secondary graphitization. *J. Mater. Sci. Technol.*, 2013, 29: 406.

[13] Y. J. Liou, W. J. Huang. Determination of graphene sheets content in carbon materials by Raman spectroscopy. *J. Chin. Chem. Soc.* 2014, 61: 1045.

[14] Yan-Jia Liou, Wu-Jang Huang. The role of sodium ions on the development of micro-sized pores in a high alpha-cellulose content woody biomass under ambient temperature. *J. Cleaner Product*. 2014, 47: 199.

[15] Y. J. Liou, W. J. Huang. Relationship between the formation of graphene fraction and the development of surface electro-conductivity of pyrolized monocotyledonous and dicotyledonous plants. *J. Cryst. Growth*. Under review.

[16] http://big5.mofcom.gov.cn/gate/big5/price.mofcom.gov.cn/channel/priceinfo.shtml?prod_id=0111651.